AN ANALYSIS OF THE EFFECTS OF GEOMETRIC SPACING ON ANTENNAS

Department of Electrical & Computer Engineering,
University of Arizona, Tucson, AZ 85721

This Paper was written in accordance to the final project requirements of ECE584 Antenna Theory and Design

John Claus

04/20/2018

Abstract – One of the simplest antennas used today is the Uniform Linear Array (ULA). This type of array is one with identical elements which all have identical magnitude and each with a progressive phase [1]. In order to improve directivity and bandwidth many times these linear arrays can modified so that their individual elements have different phase and amplitude. This project explores the effects of these modifications by analyzing a 12 and 24 element ULA and comparing it to two Flat-Top Non-Uniform Linear Arrays designed in Reference [2]. Additionally, in this project, a 900 MHz Planar Inverted F-Antenna is modified geometrically to have resonance at 815 MHz using HFSS software.

Introduction

This project is divided into three components: Part 1 – ULA Simulation, Part 2 – Flat-top Simulation, and Part 3 – 815 MHz PIFA. These topics are then broken down further into their design and their analysis components. The ULA simulation's design is created in MATLAB and is verified by comparing the simulator's output to that of equations used in Reference [1] all in the MATLAB environment. The Flattop simulator is a slightly modified version of the simulator used in Part 1 where the amplitude and phase of each induvial element can be modified independently. A first comparison is made in Part 2 of two distinct types: a 10-element array and a 12-element array [2]. A second comparison is then done of the 12-element ULA arrays' and 12-element Flattop Arrays' directivity, beam width, and number of sidelobes with respect to variations in distance length, d, between the elements in the array. Similarly in Part 3, a PIFA antenna originally configured in HFSS for resonance at 900 MHz (See Figure A) is experimentally modified by its shape to resonate at 815 MHz

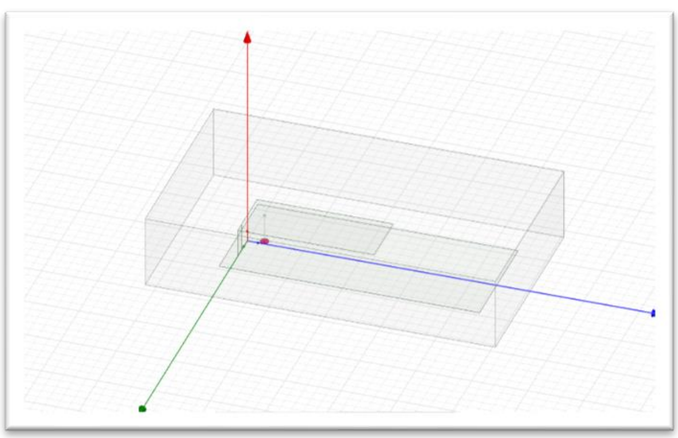

FIGURE A – HFSS graphic of the original 900 MHz PIFA

Part 1 – ULA simulation

Design

The ULA antenna simulator first calculated the array factor, AF, using equation 1.1 [1 – EQN 6.7]. This was done iteratively in a FOR loop N times where N is the number of elements in the array.

$$AF = \sum_{n=0}^{N} e^{j(n-1)\psi} \qquad EQN\ 1.1$$

The variable ψ is an equation representing the phase as a function of θ as can be seen in equation 1.2. [1 – EQN 6.7a] The variable β was set to zero for the ULA.

$$\psi = kd\ cos\theta + \beta \qquad EQN\ 1.2$$

The radiation intensity, U(θ), was then calculated using equation 1.4 [1- EQN 6-30] by squaring the normalized array factor, AFn, which was calculated by dividing the array factor by N. (See equation 1.3)

$$AF_n = {}^{AF}/_{N} \qquad EQN\ 1.3$$

$$U(\theta) = [AF_n]^2 \qquad EQN\ 1.4$$

The directivity of the ULA was then calculated (See equation 1.6) from the maximum value of the radiation intensity, U_{max} using the max() function and the calculated radiated power (See equation 1.5). It should also be noted that the change in angle, dθ, was set at 1/100th degrees.

$$P_{ave} = 2\pi \sum_{\theta=0}^{\pi} sin\theta d\theta \qquad EQN\ 1.5$$

$$D = \frac{4\pi U_{max}}{P_{ave}} \qquad EQN\ 1.6$$

The Half Power Bandwidth (HPBW) was found by the simulator through measuring the distance between the two radiation intensity values equidistant from the maximum value. The sidelobe peak values were found by using the findpeaks() function in MATLAB and their correlating angle values where then inferred from their index. As mentioned earlier, the simulation was ran using a level of precision of 1/100th degrees where 0 to 180 degrees was represented by 18,000 data points / index values.

Analysis

In order to verify that this simulator was functioning properly, it was necessary to compare its output to a calculated equivalent. This verification was done by comparing the output values for two different ULA antennas: a 12-element (See Figure 1.1) and a 24-element array. (See Figure 1.2) Additionally, a table was constructed of all the sidelobe angles and radiation intensities in dB. (See Table 1.1)

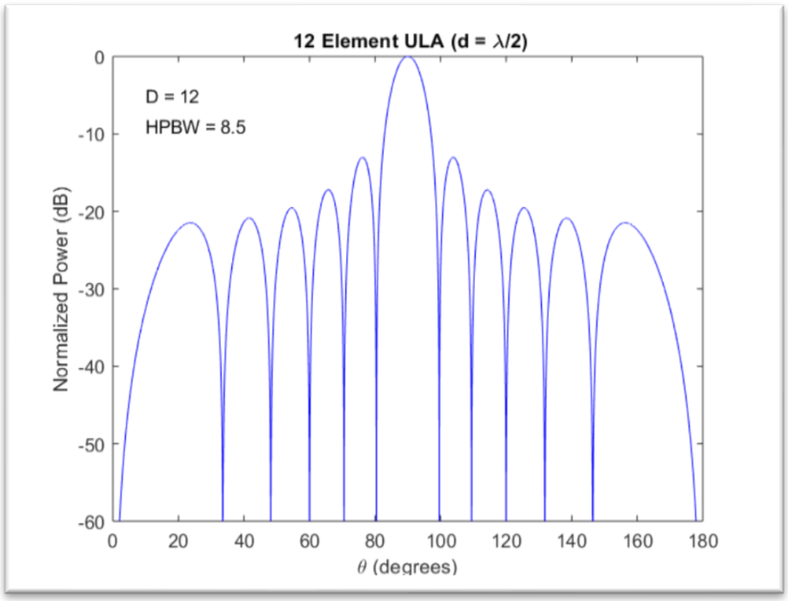

FIGURE 1.1 – 12-element ULA

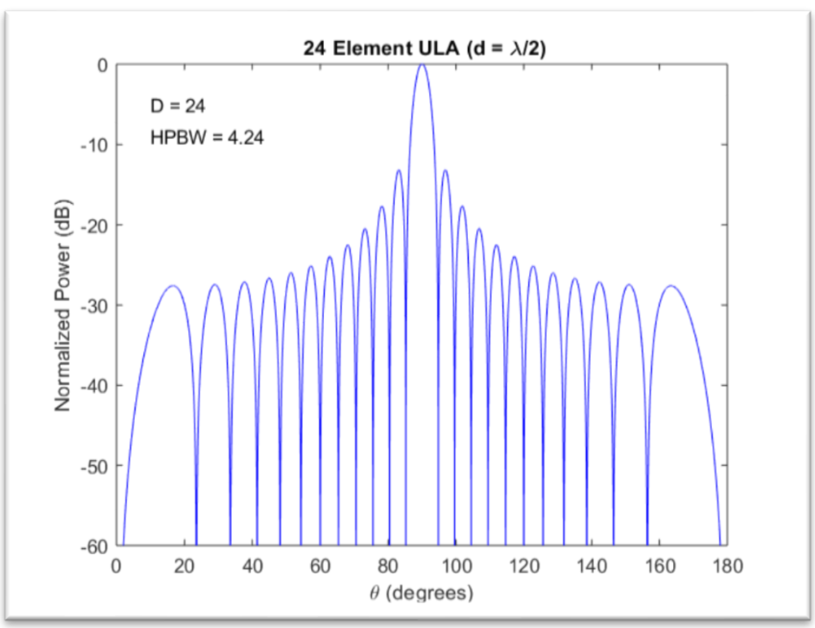

FIGURE 1.2 – 24-element ULA

12-Element Uniform Linear Array Sidelobe Intensity U(θ)										
θ (deg)	23.64	41.57	54.56	65.74	76.18	103.82	114.26	125.44	138.43	156.36
U(dB)	-21.51	-20.89	-19.56	-17.22	-13.06	-13.06	-17.22	-19.56	-20.89	-21.51

24-Element Uniform Linear Array Sidelobe Intensity U(θ)											
θ (deg)	16.61	28.98	37.69	44.94	51.37	57.27	62.80	68.08	73.18	78.17	83.15
U(dB)	-27.59	-27.44	-27.13	-26.66	-26.00	-25.12	-23.98	-22.48	-20.49	-17.68	-13.21
θ (deg)	96.85	101.83	106.82	111.92	117.20	122.73	128.63	135.06	142.31	151.02	163.39
U(dB)	-13.21	-17.68	-20.49	-22.48	-23.98	-25.12	-26.00	-26.66	-27.13	-27.44	-27.59

TABLE 1.1 – Sidelobe Values

It is clear from the graphs that increasing the number of elements increased the directivity, decreased the HPBW, and increased the number of sidelobes. This information needed to be verified as correct, therefore a comparison was made between the simulator's output and calculated approximations from Reference 1. The output values used for comparison with a calculated equivalent were the Directivity, HPBW, and peak sidelobe angle and radiation intensities in dB. (See Table 1.2) Equation 1.7 was used to calculate the Directivity [1 - EQN 6-44].

$$D_0 = 2N\frac{d}{\lambda} \qquad EQN\ 1.7$$

Equation set 1.8 was used to calculate the HPBW [1 – EQN 6-13, 6-14a, 6-14c].

$$\theta_m = \cos^{-1}\left(\frac{\lambda\beta}{2\pi d}\right) \qquad EQN\ 1.81$$

$$\theta_h = \frac{\pi}{2} - \sin^{-1}\left[\frac{\lambda}{2\pi d}\left(-\beta \pm \frac{2.782}{N}\right)\right] \qquad EQN\ 1.82$$

$$\Theta_h = 2|\theta_m - \theta_h| \qquad EQN\ 1.83$$

Equation 1.9 was used to calculate the peak sidelobe angles [1 - EQN 6-16a].

$$\theta_s = \cos^{-1}\left[\frac{\lambda}{2\pi d}\left(-\beta \pm \frac{3\pi}{N}\right)\right] \qquad EQN\ 1.9$$

Equation set 1.10 was used to calculate the peak sidelobe radiation intensities in dB. [1 - EQN 6-7a, 6-17, 6-17a]

$$\psi = kd\ cos\theta + \beta \qquad EQN\ 1.10.1$$

$$(AF)_n = 20\log_{10}\left[\frac{\sin\left(\frac{N}{2}\psi\right)}{\frac{N}{2}\psi}\right] \qquad EQN\ 1.10.2$$

As can be seen in Table 2, the simulator's output was well within an acceptable 5% margin of error to that predicted with the calculations. The largest error exists in the peak sidelobe radiation intensity values. This error is still on 3% where the rest of the simulator's outputs are less than 1% different than the calculated values for the 12-element array. It also should be noted that the simulator became more accurate as additional elements were added. Therefore, it is a relatively correct assumption that this simulator worked properly.

	12 - Element Array			24 - Element Array		
	Simulation	Calculated	Error (%)	Simulation	Calculated	Error
Directivity (D)	12.00	12.00	0.00%	24.00	24.00	0.00%
Sidelobe 1 (θ_1)	76.18	75.52	0.87%	83.15	82.82	0.40%
Sidelobe 2 (θ_2)	103.82	104.48	0.63%	96.85	97.18	0.34%
Sidelobe dB	-13.06	-13.47	3.04%	-13.21	-13.46	1.86%
HPBW (Θ_h)	8.50	8.46	0.47%	4.24	4.23	0.24%

TABLE 1.2 - Simulated vs. Calculated Results

Part 2 – Flattop simulation

Design

Once it was determined that the simulator was functionally correct when modeling a ULA, it was slightly modified to verify the results of the paper in Reference 2 for two separate Non-Uniform Linear Arrays whose output was a flat-topped pattern. This was done by modifying the AF equation (See equation 2.1) for such a design where each element had its own unique amplitude, a_n.

$$AF = \sum_{n=0}^{N} a_n e^{j(n-1)\psi} \qquad EQN\ 2.1$$

Only two examples in the paper were simulated, a 10-element array and a 12-element array with varying amplitudes as can be seen in Table 3.

N	10-Element Flattop a_n	12-Element Flattop a_n
1	1.949	1.000
2	3.433	-0.162
3	4.076	-1.177
4	2.976	-0.485
5	0.786	2.650
6	-0.966	5.790
7	-1.256	5.790
8	-0.392	2.650
9	0.496	-0.485
10	1.000	-1.177
11		-0.162
12		1.000

TABLE 2.1 – Flattop Non-Uniform Linear Array

The two arrays differ in that the 12-element array symmetric and the 10-element array has specific unique values for each amplitude. As can be seen in Figure 2.1 and 2.2, despite these differences, the patterns are almost identical.

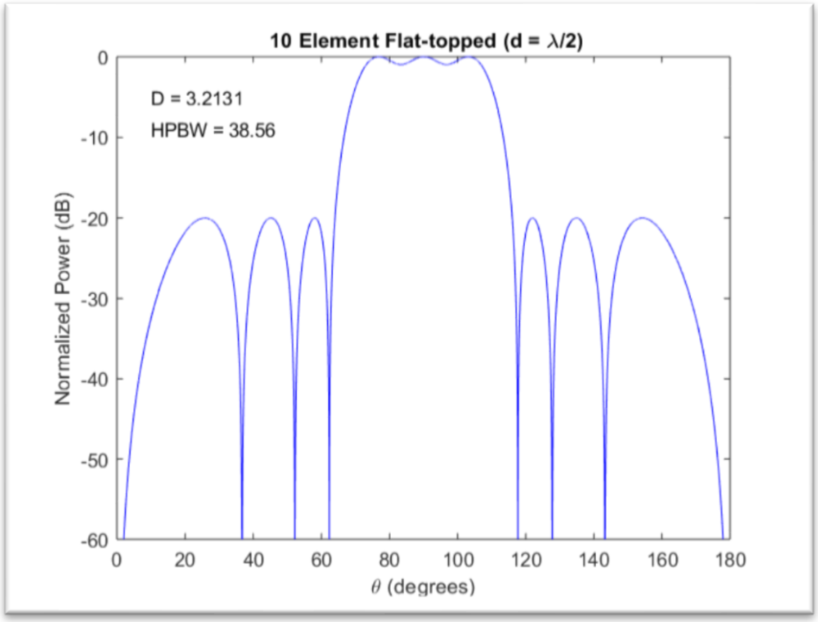

FIGURE 2.1 – 10-Element Flattop Array

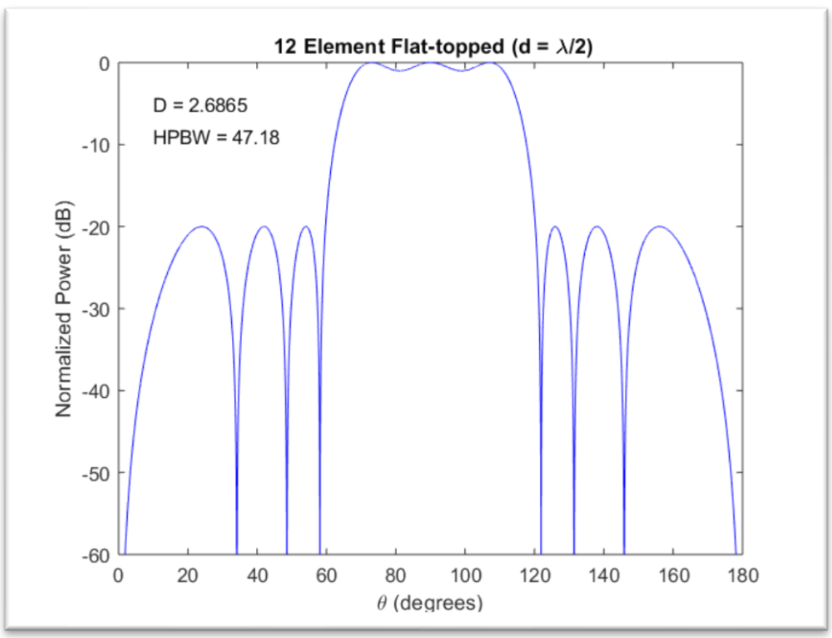

FIGURE 2.2 – 12-Element Flattop Array

Analysis

A comparison was then done between the 12-element ULA array and the 12-element flattop array where differences in the Directivity, HPBW, and the number of sidelobes between the two arrays as distance, d, was both increased and decreased in relation to the wavelength, λ. Table 2.2 outlines the changes to these values as the distance is varied.

12-Element Array Comparison			
Spacing	λ	λ/2	λ/4
	Directivity		
ULA	12	12	6.162
Flattop	2.687	2.687	1.352
	HPBW		
ULA	29.28	8.5	17.04
Flattop	71.76	47.18	106.32
	Number of Sidelobes		
ULA	21	10	4
Flattop	13	6	0

TABLE 2.2 – Variations in Spacing for 12-Element Arrays

At first glance, the differences seen in the patterns for both arrays follows what would expected for the Directivity and HPBW when shortening the distance to λ/4. However, this does not hold true for the lengthening it to λ. This is due to that metric being the measure a new dominant beam located at 0 degrees instead of 90 for both arrays. This can be seen in Figure 2.5. The number of sidelobes does increase as linear function of the distance however for both a shortening and lengthening of the spacing, d. This can be seen Figure 2.3 through 2.5.

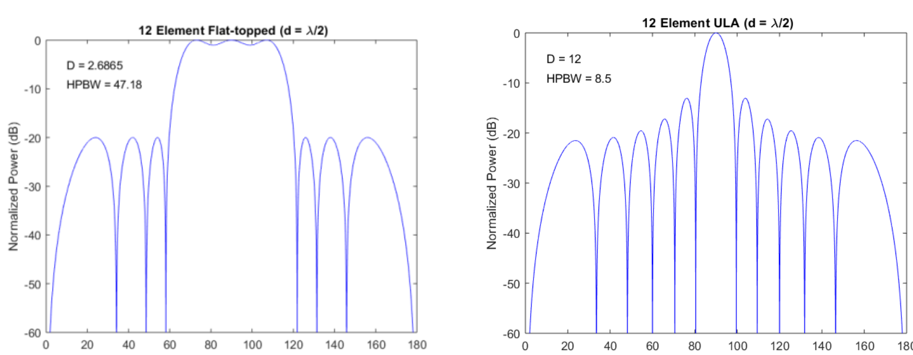

FIGURE 2.3 – Normalized Power at λ/2

It is clear that the flat-topped array has a much larger HPBW by design than the ULA. This of course limits the directivity of the signal however.

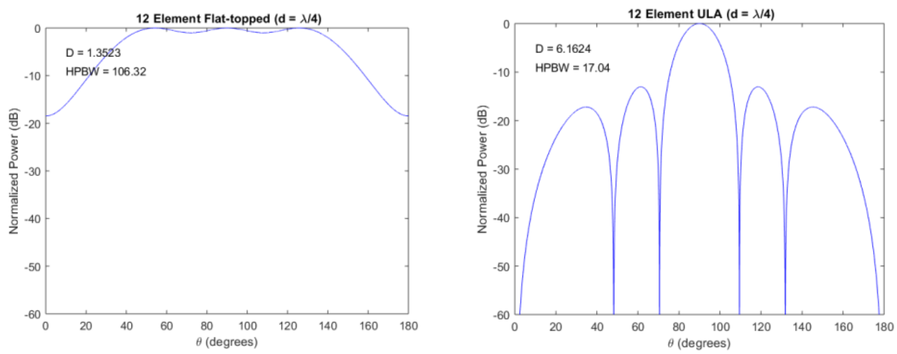

FIGURE 2.4 – Normalized Power at λ/4

The graphs here indicate that as the distance is shortened, the HPBW increases and the directivity and the number of sidelobes decrease significantly. The HPBW is so great for the flattop array that it nearly becomes an isotropic radiator at that spacing.

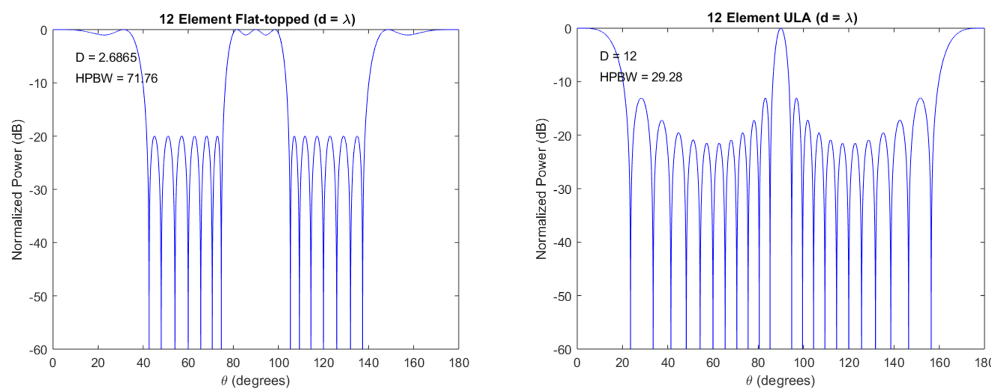

INSERT FIGURE 2.5 – Normalized Power at λ/4

As the spacing increasing to be the same as the wavelength, one would likely predict that the directivity and the number of sidelobes would further increase and the HPBW would further decrease. This does hold true for the original beam at 90 degrees. However, a new dominant beam forms at 0 degrees which interestingly affects the directivity just enough to make it exactly equal to the directivity for half of a wavelength. Additionally, the HPBW of the now dominant beam is larger than that for the beam at 90 degrees for λ/2. However, the number of sidelobes still increase as expected.

Part 3 – 815 MHz PIFA

Design

A further exploration into the effects of geometry on an antenna's performance was done with a PIFA antenna in the ANSYS HFSS modeling software. Here a PIFA antenna that had resonance at 900 MHz was modified geometrically to resonant instead at 815 MHz. Table 3.1 displays the original specifications of this planar antenna at 900 MHz in relation to the modified values for 815 MHz.

Frequency	Width	Length	dB
900 MHz	25.81	60.75	-34.25
815 MHz	26.5	68.5	-31.79

TABLE 3.1 – PIFA Antenna Specifications

These were values were experimentally calculated by recursively modifying the dimensions slightly until the resonance was found to be at 815 MHz. The largest value length was initially modified until the antenna was close, then the width was modified until the antenna behaved as desired. It was also necessary to change the step interval so that the simulation in the program could test at 815 MHz. The setting for the 900 MHz was initially set at 10 MHz increments which would only allow for 820 MHz or 810 MHz to be seen. Figure 3.1 is graphic of the functional 815 MHz PIFA antenna.

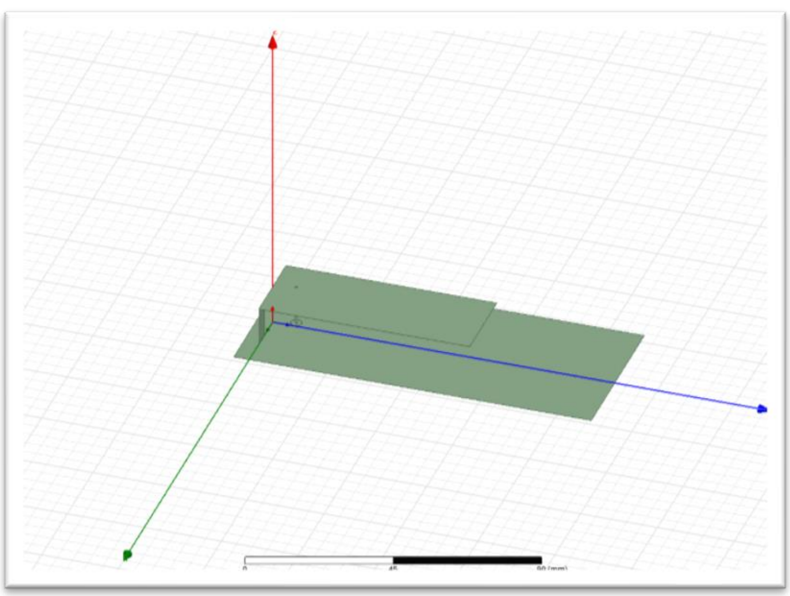

FIGURE 3.1 – 815 MHz PIFA Antenna

Analysis

Once the design was completed and a final simulation of the antenna was ran, a graph of the antenna response to the software's simulation was composed verifying that the antenna did resonate at 815 MHz.

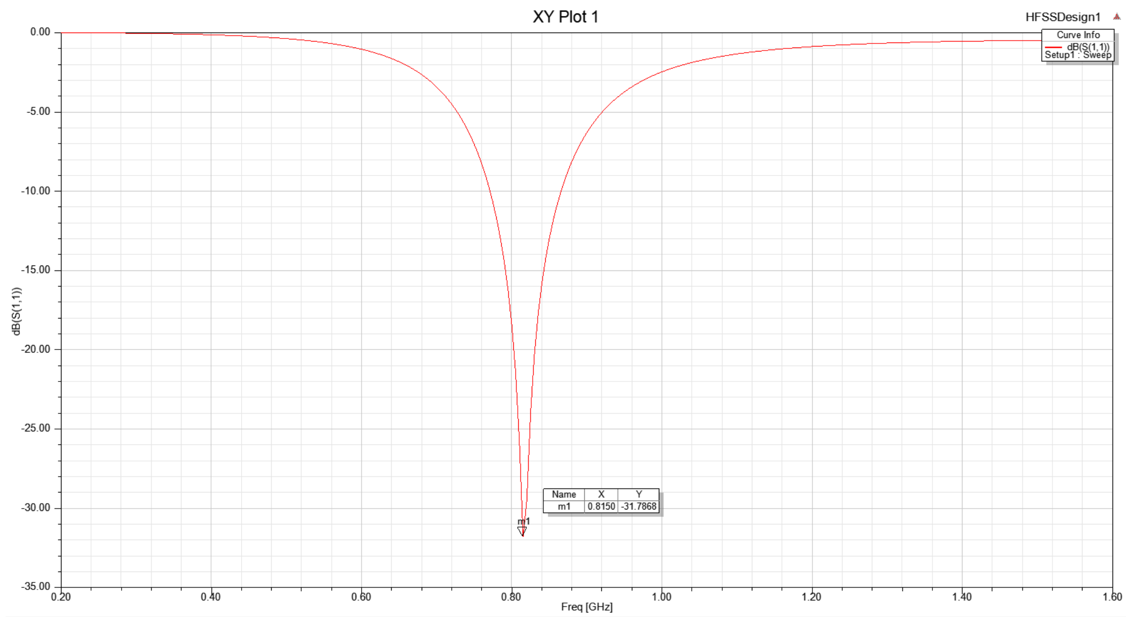

INSERT FIGURE 3.2 – Frequency Response of the 815 MHz PIFA Antenna

Conclusion

It is clear from the results of this project that geometry plays a significant role in the performance of an antenna. This hold true for all types of antennas and very modest modifications can have serious implications their performance. This is due to the geometric nature of the E & M waves to begin with. The wavelength of which is directly proportional to the frequency. Since an antenna receives and transmits this radiation, it must be matched geometrically to the wavelength for optimal performance.

References

[1] Balanis, Constantine A.. Antenna Theory: Analysis and Design (Kindle Locations 10485-10486). Wiley. Kindle Edition.

[2] Y. U. Kim and R. S. Elliott, "Shaped Pattern Synthesis using Pure Real Distributions," IEEE Transactions on Antennas and Propagation, Vol. 36, No. 11, Nov. 1988, pp. 1645-1649.